

Coherent optical and acoustic phonon generation correlated with the charge-ordering phase transition in $\text{La}_{1-x}\text{Ca}_x\text{MnO}_3$

D. Lim,¹ V. K. Thorsmølle,¹ R. D. Averitt,¹ Q. X. Jia,¹ K. H. Ahn,² M. J. Graf,¹ S. A. Trugman,¹ and A. J. Taylor¹

¹*Los Alamos National Laboratory, Los Alamos, New Mexico 87545, USA*

²*Advanced Photon Source, Argonne National Laboratory, Argonne, Illinois 60439, USA*

(Received 29 October 2004; revised manuscript received 14 January 2005; published 8 April 2005)

We have observed coherent optical and acoustic phonon generation, which are strongly coupled to the charge-ordering (CO) transition in $\text{La}_{1-x}\text{Ca}_x\text{MnO}_3$ ($x=0.5, 0.58$) using femtosecond optical pump-probe spectroscopy. Coherent optical phonons, observed at low temperatures, disappear above the charge-ordering temperature T_{CO} , while coherent acoustic phonons display the opposite behavior, disappearing gradually below T_{CO} . Coherent optical phonons are generated by the displacive excitation mechanism where their coupling to the photoexcited charge carriers is enhanced by the structural change corresponding to the CO phase transition. The oscillation frequency for the coherent acoustic phonon depends on the probe wavelength, which is consistent with the propagating strain pulse mechanism. The dramatic change of lattice constants across the charge-ordering transition explains the overall temperature dependence of the coherent acoustic phonon amplitude.

DOI: 10.1103/PhysRevB.71.134403

PACS number(s): 75.47.Lx, 78.47.+p, 71.38.-k, 63.20.Kr

I. INTRODUCTION

The hole-doped manganites $R_{1-x}A_x\text{MnO}_3$ (where R is a trivalent rare-earth ion and A is a divalent alkaline earth) with perovskite structure have been intensively studied since the rediscovery of colossal magnetoresistance in these compounds.¹ These materials offer rich physical phenomena including various magnetic phases, the metal-to-insulator transition, and charge-orbital ordering. This is due to the strong coupling of electronic, magnetic, and lattice degrees of freedom in these compounds. Under optimal hole doping ($0.17 < x < 0.5$), manganites such as $\text{La}_{1-x}\text{Ca}_x\text{MnO}_3$ undergo an insulator-metal transition with a ferromagnetic ground state.² On the other hand, highly doped manganites with $x > 0.5$ display orbital and charge order below the charge-ordering (CO) temperature T_{CO} with an antiferromagnetic ground state.^{3,4} Furthermore, the coupling of the electronic and lattice degrees of freedom as well as the interplay between the metallic and the CO phase in manganites have been studied, revealing that short-range CO correlations can exist even above the CO transition temperature.⁵

Optical spectroscopy has proven to be a useful tool in unraveling the competition between the charge, orbital, lattice, and spin degrees of freedom in such technologically relevant doped transition-metal oxides and their undoped parent compounds. An example is the charge-ordering manganite $\text{La}_{1-x}\text{Ca}_x\text{MnO}_3$, where recent optical conductivity measurements reveal short-range charge-ordering fluctuations and the development of an optical gap at temperatures below the charge-ordering temperature T_{CO} .⁶ Femtosecond optical spectroscopy complements conventional optical methods since the electron, phonon, and spin dynamics can be directly resolved in the time domain.⁷ For example, the evolution of the charge and orbital degrees of freedom in the charge-ordering manganites, following optical excitation, has been successfully studied using optical pump-probe

spectroscopy.^{8,9} However, these experiments were performed with high laser pump fluences, leading to complete melting of the charge-orbital ordering and the formation of long-lived intermediate metastable states. Also, due to the relatively long pulse duration, it was not possible to generate and detect the coherent excitation of lattice or charge order. Here, we present a low-fluence ultrafast optical pump-probe study of coherent optical and acoustic phonons coupled to the charge- and orbital-ordered phases of $\text{La}_{1-x}\text{Ca}_x\text{MnO}_3$ ($x=0.5, 0.58$).

II. EXPERIMENT

$\text{La}_{1-x}\text{Ca}_x\text{MnO}_3$ (LCMO) thin films of thickness ~ 100 nm with doping $x=0.5, 0.58$ were grown on MgO substrates by pulsed laser deposition (PLD). The PLD used a XeCl excimer laser. The substrate temperature and oxygen pressure for LCMO growth were initially optimized in terms of structure and resistivity, and were maintained at 825 °C and 400 mTorr, respectively. Highly crystalline LCMO films on MgO were confirmed by x-ray diffraction θ - 2θ scans, rocking curves, and pole figures. Samples grown by laser-pulse deposition method have been known to have a high structural quality beyond the ~ 2 -nm thick interfacial layer, and also possess bulklike macroscopic properties.¹⁰ The sample was placed inside a liquid-He-cooled cryostat with temperature capability from 7 to 400 K. Short ~ 35 -fs pulses centered at 800 nm from a Ti:sapphire oscillator were split using a beam splitter into pump and probe arms. The pump-induced change in the reflectance ($\Delta R/R$) of the sample was measured as a function of a pump-probe delay time using a mechanical delay line. In the experiments, the pump and probe beams were cross polarized to minimize coherent artifacts and noise due to pump scatter. The pump fluence was kept below $20 \mu\text{J}/\text{cm}^2$ to prevent irreversible melting of the charge ordering. To study the probe wavelength dependence, a tunable optical parametric ampli-

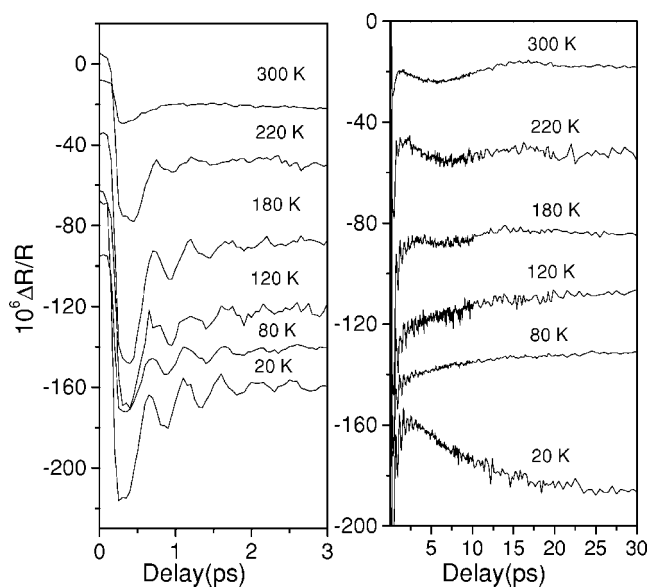


FIG. 1. Periodic oscillation in the photoinduced change in reflectivity of LCMO for $x=0.58$. The sample with $x=0.5$ is not plotted, but shows a similar behavior. The pump and probe were set to 800 nm.

fier operating at a 250-kHz repetition rate was used in a separate setup.

III. RESULTS AND DISCUSSION

In Fig. 1, pump induced changes in the differential reflectance $\Delta R/R$ as a function of pump-probe delay are plotted for $\text{La}_{1-x}\text{Ca}_x\text{MnO}_3$ ($x=0.58$) with increasing temperature. We clearly observe periodic oscillations with periods of hundreds of femtoseconds and tens of picoseconds for some of the temperatures. At low temperatures, the oscillation with period (frequency) of ~ 450 fs (~ 74 cm^{-1}) can be observed quite clearly. These oscillations are short lived, dephasing in a few picoseconds. Interestingly, when we increase the temperature of the sample, this oscillation disappears within the given signal-to-noise ratio. The amplitude of the periodic oscillation is plotted in Fig. 2 for both samples. With increasing temperature, both show an abrupt decrease of the oscillation amplitude in the vicinity of the charge-ordering temperature, although the change is more abrupt for the $x=0.58$ sample. This indicates a strong coupling of the periodic oscillation to the underlying charge-ordering phase transition.

The slower oscillation period of ~ 18 ps exhibits the opposite temperature-dependent behavior upon crossing T_{CO} . The slower oscillation, not observable at low temperatures in the CO phase, appears at approximately 100 K, and increases steadily until it saturates as can be seen in Fig. 3. Interestingly this oscillation disappears rather suddenly around 20 ps delay.

A. Coherent optical phonon generation coupled to charge-ordering transition

We will discuss the faster periodic oscillation which is strongly coupled to the charge-ordering transition first. In the

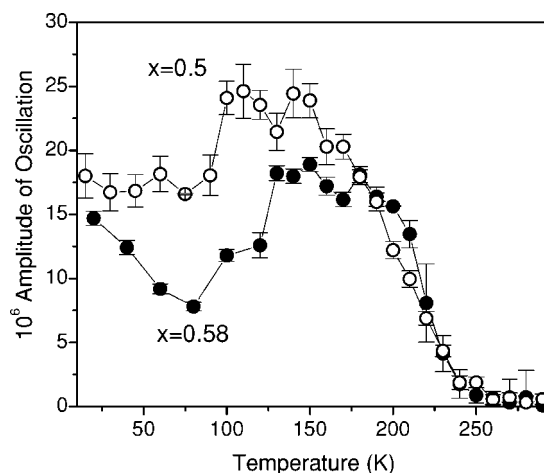


FIG. 2. The amplitude of the optical phonon oscillation as a function of temperature for $x=0.5$ (open circle) and $x=0.58$ (solid circle). The change of the amplitude for $x=0.58$ happens more rapidly than for $x=0.5$.

charge-ordered phase, there are many collective excitations which might be excited by a short optical pulse, such as phonons, charge-density waves, magnons, or the recently claimed orbiton.¹¹ The excitation frequency of charge-density waves is much lower than the one observed in our experiment and can be observed only at lower temperatures. Magnon excitation is not likely since it simply cannot persist up to the temperatures we have measured. On the other hand, coherent phonon generation is a definite possibility and it has been observed in many transition-metal oxides.

Coherent optical phonons, which appear in pump-probe spectroscopy, are Raman active. Therefore, if our data are related to coherent optical phonon generation, the corre-

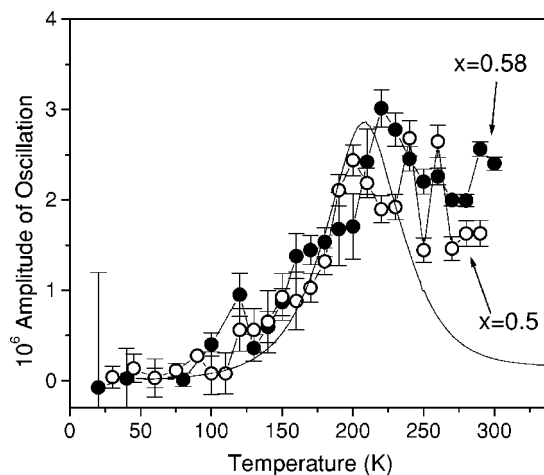


FIG. 3. The experimental results of the slow oscillation amplitude (acoustic phonons) as a function of temperature for $x=0.5$ (open circle) and $x=0.58$ (solid circle). The calculated coherent acoustic phonon amplitude, up to a scaling factor, for $x=0.5$ (solid line) uses the strain pulse model (Ref. 20), the reported change of lattice constant b (Ref. 4), and measured specific-heat data (Ref. 24) of LCMO ($x=0.5$) with $T_{\text{CO}} \approx 180$ K. Here we rescaled the temperature axis to ~ 200 K, to adjust for the difference of measurements between down vs up sweep of temperature.

sponding optical phonon mode should show up in conventional Raman spectra. Indeed, an A_g Raman mode with a similar frequency has been observed in many doped manganites that have an orthorhombic structure.^{12–16} Specifically for half-doped $\text{Nd}_{0.5}\text{Sr}_{0.5}\text{MnO}_3$, it was reported that the Raman mode appeared only below T_{CO} , together with several other A_g phonons.¹⁴ It has been proposed to be related to the structural change across the CO phase transition from the high-symmetry space group $Imma$ to $P2_1/m$ (often simplified to $Pmma$). If this is the case for our experimental results, then the sudden onset of an A_g mode of coherent optical phonon is related to the lowered symmetry in the charge-ordered phase. However, it is feasible that this A_g mode is not related to the doubling of the unit cell, since in $\text{La}_{0.7}\text{Ca}_{0.3}\text{MnO}_3$ a similar low-frequency A_g mode exists even when no charge ordering occurs.^{15,16} Therefore the A_g optical phonon mode could be Raman active at all temperatures for hole doped LCMO, and the onset of the A_g mode does not necessarily come from a simple symmetry change.

Here we discuss a generation mechanism of coherent optical phonons through a structural change induced by the charge ordering. For LCMO above T_{CO} , the tilt of the MnO_6 octahedra and Jahn-Teller distortion form a superstructure of the cubic perovskite structure. Of the total 60 Γ -point phonon modes, only 24 ($7A_g + 5B_{1g} + 7B_{2g} + 5B_{3g}$) are Raman active. In the low-temperature CO phase, charge is ordered in the ac plane, forming a superstructure with doubled lattice parameters (space group $P2_1/m$). In analyzing the Raman modes of this low symmetry phase, octahedral tilts were often ignored to make the analysis possible. This simplified structure (space group $Pmma$), has 21 Raman-active phonon modes ($7A_g + 2B_{1g} + 7B_{2g} + 5B_{3g}$) compared to the 54 Raman-active modes of the lower symmetry space group $P2_1/m$.¹²

The A_g phonon mode, observed in our experiment, has been interpreted as a rotating (external) mode of the MnO_6 octahedra.¹¹ But a Raman study using oxygen isotopes showed almost no change of the frequency with respect to the isotope, and it was proposed that the phonon mode is related to the vibration of the cation (La) in the z direction rather than the rotating mode.¹⁵

The question remains as to what is responsible for the strong correlation between the CO transition and coherent optical phonon generation. We believe that it is the structural change accompanying the charge ordering and the rearrangement of atoms within the unit cell. The structural change of the manganite $\text{La}_{0.5}\text{Ca}_{0.5}\text{MnO}_3$ studied by x-ray diffraction shows that the CO transition is accompanied by a dramatic change of the lattice parameters along all three axes.⁴ Although the transition itself is believed to be first order, the lattice constants a , c increase while b decreases over a broad temperature range, 150–240 K possibly due to sample inhomogeneity. Furthermore, the region of the steepest change displays a continuous distribution of lattice parameters, or possibly mixed phases. During this structural change, equilibrium atomic positions change dramatically, displacing Mn^{4+}O_6 octahedra (Δz) and La ($\Delta z'$) atoms.

Displacive excitation of coherent phonons (DECP) has been observed in many materials including high- T_c superconductors.^{17,18} When a short laser pulse creates electrons and holes in the charge-ordered manganites, electrons

are excited from the Mn^{3+} to Mn^{4+} sites and the positions of the atoms are no longer in equilibrium. Since charge ordering is coupled to the rearrangement of atoms, the coupling of the photoexcited electrons and the lattice forces the atoms to move to new equilibrium positions, thus triggering the coherent motion of Mn, O, and La. In this way, the optical coherent phonon with A_g mode (La atoms moving in the z direction) can be coherently excited. Other coherent phonons of A_g symmetry can also be initiated through the same mechanism, but their frequencies are too high to be observed in our experiment.

The strength of coupling of the excited carriers and the A_g phonon mode should strongly depend on the displacements of internal positions of the atoms due to the charge-ordering transition. This explains a striking similarity between the amplitude of the coherent phonon oscillations observed in our experiment and the structural change upon passing through the charge-ordering transition.⁴ CO transition temperatures of bulk CO manganite showed ~ 20 -K difference depending on whether the sample is heated or cooled during the measurement. The coherent optical phonon amplitude change of our $x=0.5$ sample, measured while increasing the sample temperature, is centered around 200 K, and the transition temperature is very close to that of the structural change of bulk $\text{La}_{0.5}\text{Ca}_{0.5}\text{MnO}_3$, measured while heating the sample.

Figure 2 also reveals a slight difference for samples $x=0.5$ and $x=0.58$. The change of the coherent phonon amplitude with temperature is more abrupt in the case of $x=0.58$ compared to $x=0.5$. This may indicate that there are stronger CO fluctuations in the half doped mixed manganite due to the competition between the metallic and the CO phases.

B. Coherent acoustic phonon generation coupling to the CO phase

Low-frequency impulsive excitation by short laser pulses have been observed and reported for coherent excitation of magnons,¹⁹ charge-density waves,²⁰ and acoustic phonons,^{21–24} which are all possibilities for the antiferromagnetic CO manganites. However, the slow oscillation is observed above the CO temperature, which excludes the possibility of magnetic or charge-density wave origin, since the long-range ordering disappears above T_{CO} . We will show that the slow oscillation indeed originates from coherent acoustic phonons, which follows the propagation strain pulse mechanism.

Several mechanisms of coherent acoustic phonons have been reported previously. In the propagating strain pulse mechanism, proposed by Thomsen *et al.*,²¹ a propagating strain pulse is generated by a stress gradient near the surface due to the finite absorption depth of the laser pulse. A periodic oscillation is observed in the reflectance, originating from the interference of the probe beams reflected from the interfaces defined by the crystal surface and the propagating strain pulse. The distinct characteristic of this mechanism is that the oscillation period τ_p depends on the probe wavelength—that is, $\tau_p \sim \lambda_{\text{probe}}/2n\nu_s$ (ν_s is the sound velocity, n is the refractive index at the probe wavelength). The

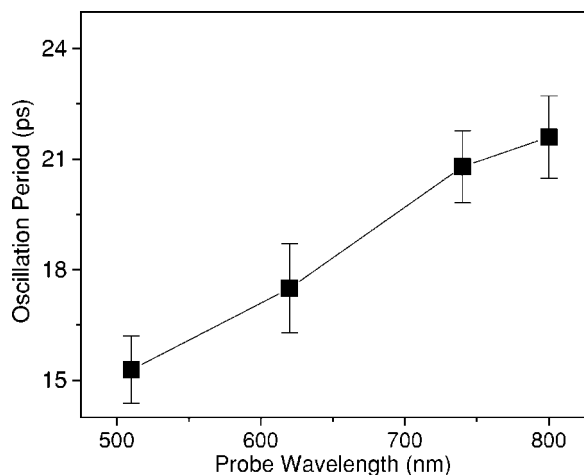


FIG. 4. Oscillation frequency vs probe wavelength for LCMO ($x=0.58$). Large fitting error bars are mainly due to the limited duration of the oscillations. The pump wavelength is 400 nm.

ballistic nature of this mechanism can be seen either by additional modulation of the oscillation, whose period depends on the film thickness or by disappearance of the oscillation, depending on whether the strain pulse is reflected by or transmitted through the underlying substrate.

Other mechanisms for the generation of coherent acoustic phonons, such as impulsive stimulated Raman scattering²² and displacive excitation of coherent phonons,²³ have been identified for bulk semiconductors and superlattices. In both cases the coherent acoustic oscillations are detected through changes in the reflection or transmission by the modulation of interband transitions coupled to the deformation potential. Large amplitude oscillations in GaN heterostructures have been observed recently and are attributed to the screening of the piezoelectric field by photoexcited carriers.²⁴ In the case of impulsive stimulated Raman scattering, the generated acoustic phonon wave vector q should be well defined, i.e., $q \sim 4\pi/\lambda_{\text{pump}}$ in the backscattering geometry. In both models, the oscillation frequency depends on λ_{pump} and not on λ_{probe} . In our experiment, the oscillation frequency does not depend on the pump wavelength. On the contrary, as shown in Fig. 4, the experimentally observed oscillation period strongly depends on the probe wavelength, indicative of the strain pulse mechanism. Furthermore, the ballistic nature of the propagating pulse mechanism is also found in the abrupt disappearance of oscillations around 20–25 ps. The time required for the generated pulse to travel the entire film thickness is $\tau_{\text{film}} \sim t_{\text{film}}/\nu_s \sim 100 \text{ nm}/5 \times 10^3 \text{ m/s} \sim 20 \text{ ps}$, which agrees with the experiment. These arguments confirm that the oscillations result from coherent acoustic phonons, which are generated at the surface and propagate through the film into the substrate.

Here we will discuss the temperature-dependent coherent phonon amplitude observed in the experiment. After photoexcitation, excited electrons and holes relax by emitting incoherent optical and acoustic phonons, and finally reach thermal equilibrium with the phonons. Both hot electrons holes and phonons, whose temperature distribution is determined by the absorption coefficient, put stress on the CO manganite

to generate coherent acoustic phonons in the form of an impulsive strain “pulse.” Calculating the stress induced by the sudden rise of the temperature of electrons and phonons is a formidable task. Here we will make an assumption that the stress is proportional to the difference of the equilibrium lattice constants at temperatures before and after optical excitation. For our experiments, the lattice parameter b , which is normal to the surface, is the most relevant parameter, since we are dealing with a strain pulse propagating in the z direction, which is coupled to stress in the b direction. So, only the temperature-dependent lattice constant b (along the z direction) will be considered in our discussion. The stress induced by photon absorption is expected to be roughly proportional to the changes in lattice constants due to the increased temperature. The manganites that we have studied have an orthorhombic structure below the charge-ordering temperature with three lattice constants, $a \sim 2\sqrt{2}a_0$, $c \sim 2\sqrt{2}a_0$, $b \sim 2a_0$, where a_0 is the basic Mn-Mn distance of about 4 Å.¹¹ The temperature dependence of the three lattice constants is most prominent around the charge-ordering temperature,⁴ which we believe is the origin of the large coherent acoustic phonon amplitude near T_{CO} . Since we keep the laser fluence Q constant at different temperatures, the change in temperature ΔT near the surface due to the absorption of a laser pulse, is proportional to $Q/C(T)$, where $C(T)$ is the specific heat.²⁵ Then the changes in lattice constants (for example b) due to heating $\Delta b \propto [db(T)/dT][1/C(T)]$, which is shown in Fig. 3 with a constant scale factor to fit the data. In spite of the assumptions made in the model, it reasonably reproduces the general behavior of the data: (i) a peak near T_{CO} and (ii) the disappearance of the coherent acoustic phonons at low temperatures, which comes from the vanishing of the derivative of lattice parameter b below the charge-ordering temperature. Above T_{CO} , the experimental data show signs of a decrease of the amplitude as T increases, in spite of the large scatter due to the difficulty of the measurement. This feature has been captured in the calculation, although with a more pronounced decrease.

We believe this originates from our simplified assumption. Above all, our thin film is grown on a substrate, which constrains the lattice constants a and c along the surface. This, in turn, will affect the temperature dependence of lattice constant b , making it deviate from the experimental result of a single crystal. Also, although the x-ray diffraction showed a film with the b axis pointing in the direction of the surface normal, some domains with different crystal directions can grow during the deposition of the film. The use of crystal lattice constant data on a thin-film sample may be the main reason for the discrepancy. Second, the oscillation amplitude is not just a function of the coherent acoustic phonon amplitude. The optical probe at 1.55 eV does not measure the coherent phonon amplitude directly, but through the changes in the refractive index n and the extinction coefficient k induced by the coherent acoustic phonon. Since there is significant spectral weight shift in the absorption spectrum that occurs when opening a charge-ordering gap, the effective change of n and k values at the probe photon energy for the same coherent acoustic phonon amplitude can change with temperature. This effect can mask the actual temperature de-

pendence of the coherent acoustic phonon amplitude. In any case, the overall agreement of the calculated result with the experimental data indicates that the acoustic coherent phonon generation is most likely coupled to the structural changes which occur across the CO transition.

IV. CONCLUSIONS

In conclusion, we have observed coherent acoustic and optical phonon generation, which is strongly coupled to the charge-ordering phase transition. In addition, we have described a mechanism for which a Raman-active, coherent A_g phonon mode can be generated in the CO phase by a displa-

cive excitation mechanism. On the other hand, the observed acoustic coherent acoustic phonon disappears below the charge-ordering temperature. The vanishing of the acoustic amplitude at low temperatures is in agreement with the strain pulse mechanism and highlights the strong coupling between the acoustic vibrations and the structural changes that occur across the charge-ordering transition.

ACKNOWLEDGMENT

This work was supported by the Los Alamos National Laboratory Research and Development Program and the US Department of Energy.

-
- ¹S.-H. Jin, T. H. Tiefel, M. McCormack, R. A. Fastnacht, R. Ramesh, and R. H. Chen, *Science* **264**, 413 (1994).
²P. Schiffer, A. P. Ramirez, W. Bao, and S.-W. Cheong, *Phys. Rev. Lett.* **75**, 3336 (1995).
³Jeroen van den Brink, Giniyat Khaliullin, and Daniel Khomskii, *Phys. Rev. Lett.* **83**, 5118 (1999).
⁴P. G. Radaelli, D. E. Cox, M. Marezio, and S. W. Cheong, *Phys. Rev. B* **55**, 3015 (1997).
⁵K. H. Kim, M. Uehara, and S.-W. Cheong, *Phys. Rev. B* **62**, R11945 (2000); T. Y. Koo, V. Kiryukhin, P. A. Sharma, J. P. Hill, and S.-W. Cheong, *ibid.* **64**, 220405 (2001); V. Kiryukhin, T. Y. Koo, H. Ishibashi, J. P. Hill, and S.-W. Cheong, *ibid.* **67**, 064421 (2003); K. H. Ahn, T. Lookman, and A. R. Bishop, *Nature (London)* **428**, 401 (2004).
⁶K. H. Kim, S. Lee, T. W. Noh, and S. W. Cheong, *Phys. Rev. Lett.* **88**, 167204 (2002).
⁷R. D. Averitt and A. J. Taylor, *J. Phys.: Condens. Matter* **14**, R1357 (2002).
⁸M. Fiebig, M. Miyano, Y. Tomioka, and Y. Tokura, *Appl. Phys. B: Lasers Opt.* **71**, 211 (2000).
⁹T. Ogasawara, T. Kimura, T. Ishikawa, M. Kuwata-Gonokami, and Y. Tokura, *Phys. Rev. B* **63**, 113105 (2001); T. Ishikawa, K. Ookura, and Y. Tokura, *ibid.* **59**, 8367 (1998).
¹⁰F. Giesen, B. Damaschke, V. Moshnyaga, K. Samwer, and G. A. Müller, *Phys. Rev. B* **69**, 014421 (2004).
¹¹E. Saitoh, S. Okamoto, K. T. Takahashi, K. Tobe, K. Yamamoto, T. Kimura, S. Ishihara, S. Maekawa, and Y. Tokura, *Nature (London)* **410**, 180 (2001).
¹²M. N. Iliev, M. V. Abrashev, H.-G. Lee, V. N. Popov, Y. Y. Sun, C. Thomsen, R. L. Meng, and C. W. Chu, *Phys. Rev. B* **57**, 2872 (1997); M. V. Abrashev, J. Bäckström, L. Börjesson, M. Pissas, N. Kolev, and M. N. Iliev, *ibid.* **64**, 144429 (2001).
¹³V. B. Podobedov, A. Weber, D. B. Romero, J. P. Rice, and H. D. Drew, *Phys. Rev. B* **58**, 43 (1998).
¹⁴H. Kuroe, I. Habu, H. Kuwahara, and T. Sekine, *Physica B* **316**, 575 (2002).
¹⁵V. A. Amelichev, B. Güttler, O. Yu. Gorbenko, A. R. Kaul, A. A. Bosak, and A. Yu. Ganin, *Phys. Rev. B* **63**, 104430 (2001).
¹⁶K.-Y. Choi, P. Lemmens, G. Güntherodt, M. Patabiraman, G. Ranarajan, V. P. Gnezdilov, G. Balakrishnan, D. McK. Paul, and M. R. Lees, *J. Phys.: Condens. Matter* **15**, 3333 (2003).
¹⁷H. J. Zeiger, J. Vidal, T. K. Cheng, E. P. Ippen, G. Dresselhaus, and M. S. Dresselhaus, *Phys. Rev. B* **45**, 768 (1992).
¹⁸W. A. Kutt, W. Albrecht, and H. Kurz, *IEEE J. Quantum Electron.* **28**, 2434 (1992).
¹⁹H. Kamioka, S. Saito, M. Isobe, Y. Ueda, and T. Suemoto, *Phys. Rev. Lett.* **88**, 127201 (2002).
²⁰J. Demsar, K. Biljakovic, and D. Mihailovic, *Phys. Rev. Lett.* **83**, 800 (1999).
²¹C. Thomsen, H. T. Grahn, H. J. Maris, and J. Tauc, *Phys. Rev. B* **34**, 4129 (1986).
²²A. Yamamoto, T. Mishina, Y. Masumoto, and M. Nakayama, *Phys. Rev. Lett.* **73**, 740 (1994).
²³J. J. Baumberg, D. A. Williams, and K. Kohler, *Phys. Rev. Lett.* **78**, 3358 (1997).
²⁴Chi-Kuang Sun, Jian-Chin Liang, and Xiang-Yang Yu, *Phys. Rev. Lett.* **84**, 179 (2000).
²⁵H. D. Yang, H. L. Huang, P. L. Ho, W. L. Huang, C. W. Huang, S. Mollah, S. J. Liu, and J.-Y. Lin, *Physica B* **329-333**, 801 (2003).